



CrossMark
click for updates

Cite this: *RSC Adv.*, 2015, 5, 37292

Received 23rd March 2015

Accepted 16th April 2015

DOI: 10.1039/c5ra05141j

www.rsc.org/advances

On the mechanism of the Shapiro reaction: understanding the regioselectivity†

Ignacio Funes-Ardoiz, Raúl Losantos and Diego Sampedro*

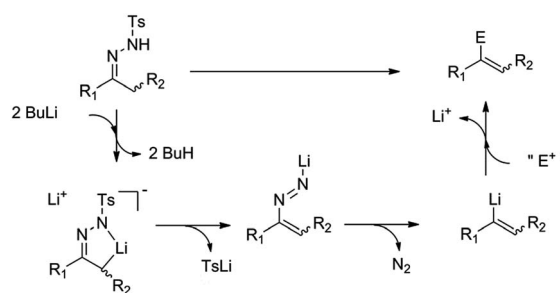
A detailed DFT-level mechanism elucidation of the two-step reaction of tosylhydrazones with alkyllithium reagents (the Shapiro reaction) is presented. A rationale of the experimental regioselectivity is offered together with some suggestions for modifying the experimental main regioisomer. Also, the proposed general mechanism was checked with a recent modification of the Shapiro reaction involving a fluorination reaction.

Introduction

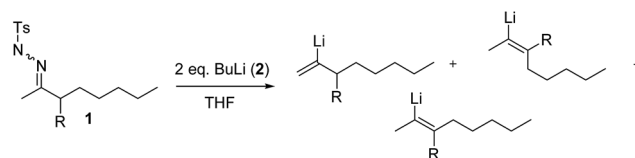
Since the first report in 1967,¹ the reaction of tosylhydrazones with alkyllithium reagents to yield alkenes (the Shapiro reaction) has been extensively employed in organic synthesis.^{2–4} In its basic form, a ketone or aldehyde is reacted to yield a tosylhydrazone that subsequently is treated with two equivalents of an alkyllithium reagent. The first equivalent is used to deprotonate the hydrazone and the second one abstracts an α hydrogen to yield a carbanion. This intermediate subsequently evolves losing the tosylate group and molecular nitrogen and producing a vinyl lithium species. In the last step, this sp^2 carbanion can be trapped with electrophiles or quenched with water or acid. The Shapiro reaction has proven to be a very efficient way to create new C–C bonds while including a vinyl functionality in the product. This versatility, the easy handling of common reagents and relatively good yields allowed for the use of the Shapiro reaction in a good number of synthesis of natural products^{5–7} including the total synthesis of Taxol^{8,9} and other substituted alkenes^{10–14} difficult to obtain by other means. In a subsequent modification¹⁵ a catalytic version of the reaction was developed in which the stoichiometric amount of base was replaced by catalytic lithium amides.

The mechanism of the Shapiro reaction has been also explored experimentally⁴ with the main aim of controlling the regioselectivity of the alkene formation. For many years, the mechanistic proposal depicted in Scheme 1 has been accepted in the literature. However, to the best of our knowledge, no detailed computational exploration of the Shapiro reaction has been performed to date and only a related reaction has been studied.¹⁶

For this reason, we selected a model reaction under common conditions to check the mechanism of the Shapiro reaction in



Scheme 1 Proposed mechanism for the Shapiro reaction.



Scheme 2 Model reaction for characterizing the mechanism.

order to clarify the origin of the regioselectivity with the ultimate aim of increasing the versatility and scope of this transformation (Scheme 2).

Here we report our results on the Shapiro reaction mechanism using the density functional theory (DFT). First, we will present a general description of the computed mechanism. Then, we will apply the computed mechanism to a recent synthetic modification of the reaction. Finally, we will suggest some experimental modifications in order to alter the product regioselectivity.

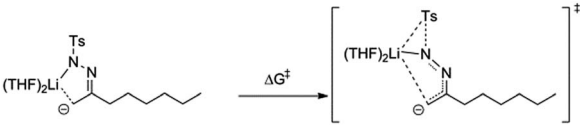
Results and discussion

Several functional and basis sets were first evaluated in order to benchmark the theoretical results. For that, we chose one of the key intermediates in the Shapiro reaction (see below) and we

Departamento de Química, Universidad de La Rioja, Centro de Investigación en Síntesis Química (CISQ), Madre, de Dios, 51, 26006 Logroño, Spain. E-mail: diego.sampedro@unirioja.es

† Electronic supplementary information (ESI) available: Cartesian coordinates for computed compounds. See DOI: 10.1039/c5ra05141j

Table 1 Functional and basis set evaluation



Functional	Basis set	$\Delta G^{\ddagger a}$	dN-S ^b
B3LYP	6-31G(d)	11.8	1.974
B3LYP	6-31+G(d)	10.0	1.965
B3LYP	cc-PVTZ	13.3	1.996
M06-L	6-31G(d)	16.1	2.034
M06	6-31G(d)	16.8	2.024
M06-2X	6-31G(d)	17.6	2.021
SVWN	6-31G(d)	13.2	2.211

^a Free energy in kcal mol⁻¹. ^b Bond length between N-S in the TS (Å).

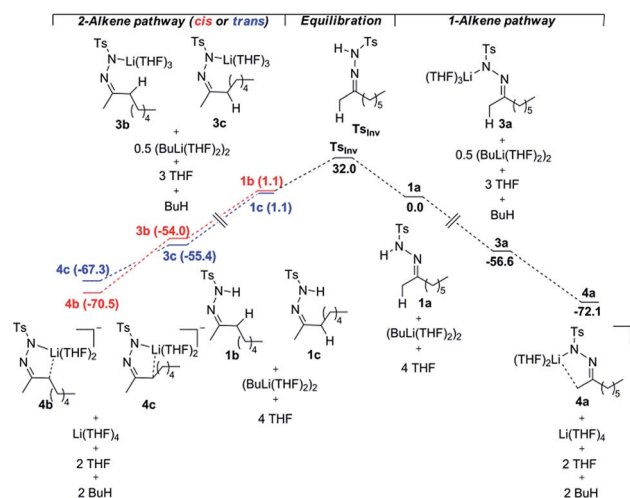
calculated the energies and geometries of the rate determining step using diverse model chemistries (Table 1).

In order to check the methodology used, we computed the tosyl dissociation step (rate limiting step, see below) with different basis sets and functionals. A small influence of the level of theory employed was found. The energy barrier can vary from 10.0 kcal mol⁻¹ to 16.8 kcal mol⁻¹. We tested the influence of the percentage of Hartree-Fock exchange in the functional (M06 family) but this effect is minor. In addition, no direct correlation between the different functionals and basis sets was found. Also it is important to note that all the energy barriers are easily affordable for a thermal process under the reported experimental conditions. Also, the computed geometries for the transition structures are slightly different. The critical N-S distance for the tosyl dissociation varies in the TSs from 1.965 Å to 2.024 Å (except the LDA functional SVWN which overestimates it by 0.2 Å). Taking into account these results, we chose the B3LYP functional and the 6-31G* standard basis set for the complete mechanism evaluation as this level of theory offers intermediate values for the energy value and the geometry of the TS at a considerably lower computational cost taking into account the large number of atoms in our system (up to 132 atoms).

In order to study the model reaction, we started by calculating the diverse deprotonation processes available for the tosylhydrazone **1** with BuLi **2**. Tosylhydrazone **1** was chosen to mimic the experimental results. The alkyl chain conformations were studied in detail in the first step and the most stable one was chosen for the subsequent steps allowing in all cases a full reoptimization. It is important to remark that lithium species in organic coordinating solvents (such as THF) form aggregates with the solvent. The exact structure and reactivity of these aggregates is a relevant issue on its own and it has been extensively addressed through theoretical calculations before.¹⁷ For instance, it has been determined that higher aggregates (tetramers) are usually dominant in solution although they are less reactive than monomers due to steric effects. While MP2 was reported to yield good results for small aggregates,¹⁸

computation of larger species seems yet unpractical at this level of theory, especially for complex reactions. In contrast, affordable DFT calculations can yield also reliable results.¹⁹ Thus, for the proper description of the intermediates, we selected as the reference structure a dimer reported by McGarrity,²⁰ which is in equilibrium with the tetramer. Based in previous calculations on related compounds,¹⁷ we assume that the dimer will be more reactive than the tetramer. Also, for the sake of energy comparison, we maintained in all points the tetracoordinated environment of the lithium atom, using explicit solvent molecules of THF. Although lithium species could be more complex, this approach allows us to compare similar structures arising from the deprotonation of the initial reactant. Therefore, throughout the paper we will take this structure as the most reactive lithiated species and we will maintain the composition of the species to allow energy comparison by computing also butane or THF in the different steps.

Initially, the tosylhydrazone **1** has three different isomers which could eventually form three different products, namely the 1-alkene and 2-alkene in *cis* and *trans* configurations (Scheme 3). In one of them, the hydrazine moiety is *syn* with respect to the terminal methyl group (**1a**, the position of the alkyl chain is irrelevant as the same terminal alkene will form) and the other two (**1b** and **1c**) are *anti* with a varying disposition of the alkyl chain. It is clear that the last two can equilibrate easily by rotation around the C-C bond, but the interconversion of the *syn* and *anti* forms of the C=N moiety is not clear. This issue has been discussed in the literature.²¹ Experimental data show that the disposition of the hydrazone is important for the outcome of the reaction. Interestingly, our model reaction provides a mixture of the internal and terminal alkene products depending on the initial proportion of these two isomers (see below). However, this functional group can equilibrate if the synthetic procedure involves acid conditions.²¹ For this reason, assuming that the hydrazone is in equilibrium, we can extract information from the deprotonated species. It should be noted that all the species shown in Scheme 3 have the same



Scheme 3 Deprotonation pathways of the tosylhydrazone **1**. Free energies in kcal mol⁻¹ referred to **1a**.

composition. Along the reaction coordinate, the connectivity is quite different in some cases but the number of atoms remains the same in all cases by computing the required compounds. Also, the tetrahedral coordination of the lithium atom is included by using THF molecules. Thus, the energies of all the species included in Scheme 3 are comparable.

In Scheme 3, we show the different possibilities that may arise. It is important to note that the regiochemistry of the reaction is determined in the first step and the relative stability of reactants **1** will control the experimental outcome. The energy difference of $1.1 \text{ kcal mol}^{-1}$ between **1a** and **1b/1c** explains the mixture experimentally obtained under equilibrium conditions. These values of free energy predict a 86 : 14 ratio, while a mixture of about 80 : 20 for the terminal alkene was experimentally found. However, it should be noted that a slight variation in the reaction conditions also allows to obtain **1** purely as the **1a** isomer. In this case (without equilibration conditions), the product will be the 1-alkene due to the isomeric stability of the hydrazone (32 kcal mol^{-1} of isomerization

barrier).²¹ Thus, although the internal deprotonation is usually favoured due to the higher acidity of the internal protons, this is not the case for **1**. Even though the internal anion is usually thermodynamically favoured, our calculations show that the *syn* dianion **4a** is the most stable ($-72.1 \text{ kcal mol}^{-1}$) compared to the *anti* conformers **4b** (-70.5) and **4c** (-67.3). We assign this behaviour to the steric interaction between the lithium environment and the alkyl chain (Fig. 1). Our results show a good agreement with the experimental data as the reaction outcome under both equilibrium conditions (in which the relative stability of the different isomers govern the regioselectivity) and non-equilibrium conditions (only **1a** is formed) is explained. However, the little differences between **4a**, **4b** and **4c** suggest that their relative stability could be controlled under the use of proper functional groups, especially if the internal protons are acid enough to be abstracted even if the hydrazone is in *anti* conformation. For this reason, we tried to develop *via* rational design a controlled version of the Shapiro reaction, increasing the acidity of the internal positions with acceptor groups (see below).

From the dianionic species **4**, a vinyl lithium intermediate is produced that can be subsequently trapped by different electrophiles such as H^+ , $\text{CH}_2=\text{O}$ or, more recently, " F^+ ".²²

Although the mechanism may appear simple, the dependence with the dianion structure is interesting in order to confirm the regioselectivity modification. The reaction starts with the loss of the tosyl group from **4** and the generation of the intermediate **5** (Scheme 4). The barrier for these processes is almost independent of the dianion structure ($11.8 \text{ kcal mol}^{-1}$ for **4a**, $9.8 \text{ kcal mol}^{-1}$ for **4b** and $10.3 \text{ kcal mol}^{-1}$ for **4c**). It suggests that once the dianion is formed, the reaction

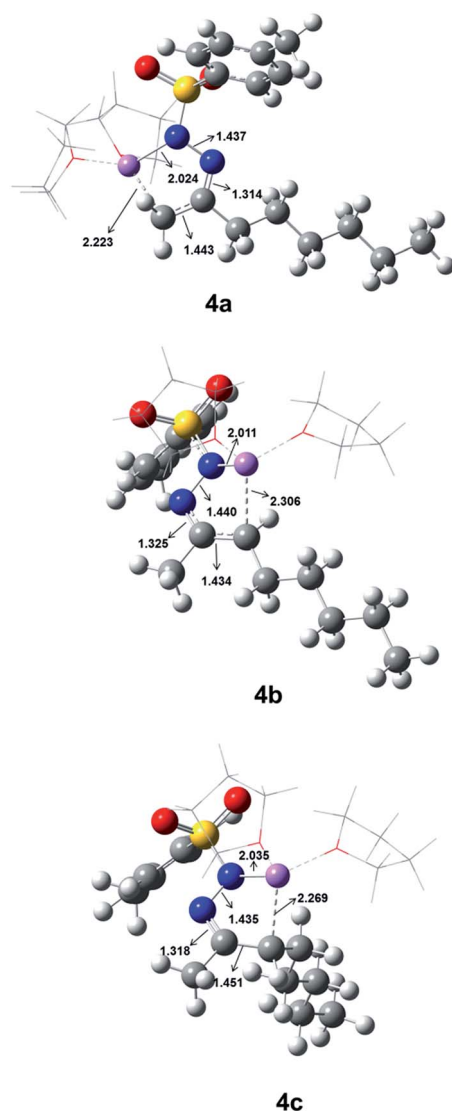
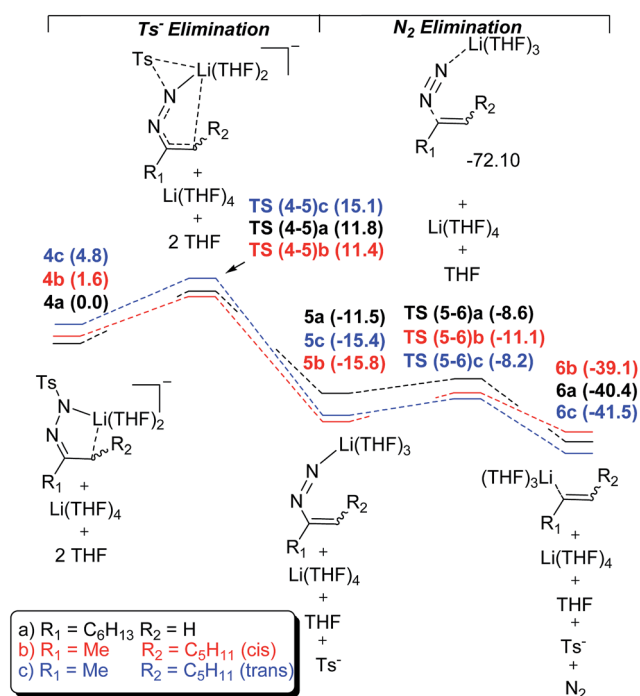


Fig. 1 Computed structures for the intermediates **4a**, **4b** and **4c**.



Scheme 4 Free energy profile of the reaction between **3** and methylpropiolate. All energies are in kcal mol^{-1} referred to **4a**.

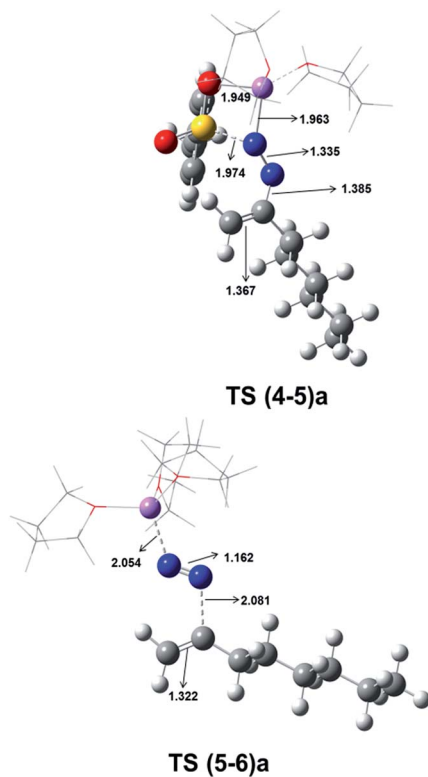
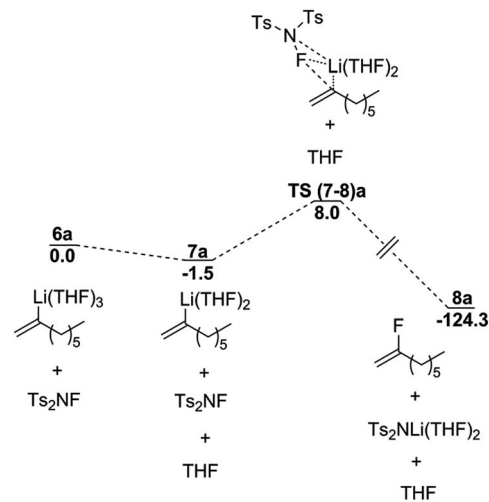


Fig. 2 Computed structures for the transition structures TS(4–5)a and TS(5–6)a.

undergoes easily this step. Interestingly, during this reaction step, the relative stability of the different regioisomers is reversed, probably due to the intrinsic stability of the internal alkenes, especially of the *trans* one. However, the small differences in energy found for the three compounds make difficult to draw definitive conclusions. After that, intermediate **5a** releases nitrogen with a small barrier ($2.9 \text{ kcal mol}^{-1}$) yielding the terminal alkene product. The barriers for the other two products are only slightly higher, 4.7 and $7.2 \text{ kcal mol}^{-1}$. Again, the composition of all the species in Scheme 4 are the same as the coordination of the lithium atoms is maintained with THF molecules when required and the tosyl group and nitrogen molecule are also included. The geometries of the computed structures for **TS(4–5)a** and **TS(5–6)a** are shown in Fig. 2.

Then, we checked this general mechanism for the recent modification of the Shapiro reaction which features an electrophilic fluoride addition.²² To do this, we computed the addition of *N*-fluorobenzenesulfonimide (NFSI) to the resulting vinyl lithium intermediate (Scheme 5). It is important to note that this reaction implies a variation of the common experimental conditions used for the traditional Shapiro reaction. Thus, it could be relevant to determine whether the mechanistic information accumulated through the years is also applicable in this specific case. As expected for the mild reaction conditions, the barrier could be easily surmountable ($8.0 \text{ kcal mol}^{-1}$). The reaction is highly exothermic ($124.3 \text{ kcal mol}^{-1}$), probably due to the intrinsic instability of the anionic vinyl group and the stability of the Ts_2N^- moiety in **8a** due to charge delocalization.



Scheme 5 Electrophilic fluoride addition to the vinyl lithium intermediates.

In contrast, other cationic electrophilic fluorides experimentally tested did not work.²² The explanation could reside in the neutralization of charges in this specific reaction while with the other reagents, a cationic lithium remains in solution.

Finally, in order to check the effect of the substituents on the regioselectivity of the reaction, we computed the suggested intermediate with different functional groups in the position 3 of the alkyl moiety. To cover a representative range of functional group properties, we selected the amino, methoxy, phenyl, cyano and nitro groups as substituents (Table 2).

As we expected, there is a clear tendency on the stability of dianions, directly related to the acidity of the internal protons. Both nitro and cyano groups favoured considerably the internal dianion formation, even with the tosylhydrazone moiety *syn* to the terminal methyl group (**12**). This implies that, in those

Table 2 Relative free energies of reactive intermediate with different substituents. Energies in kcal mol^{-1} relative to the lower energy isomer

R	9	10	11	12
NMe ₂	0.0	4.3	9.6	7.9
OMe	0.0	3.6	7.4	9.5
H	0.0	1.6	4.8	8.5
Ph	2.8	1.8	0.0	8.5
CN	25.5	1.3	9.4	0.0
NO ₂	44.2	9.2	18.7	0.0

cases, only the internal product should be formed. In contrast, donor groups such as amino or methoxy substituents disfavour considerably the internal deprotonation, increasing the selectivity of the external position. It is important to notice that in the case of cyano and nitro groups, the selectivity does not depend on the relative position of the hydrazone because the chelated intermediates (**9**, **10**, **11**) are not favoured in this case. In both cases, the species **12** are more stable, suggesting an independent deprotonation of the nitrogen and α -carbon. Thus, we conclude that the regioselectivity of the Shapiro reaction could be controlled through the acidity of this position. This fact, if confirmed by experiments, could be useful in order to further control the regioselectivity of the reaction and, in turn, to increase the interest of an already extremely powerful synthetic tool. The complex mechanism of the Shapiro reaction and the intrinsic problems associated with the computational determination of organometallic reactions suggest that these predictions should be the subject of detailed experimental exploration, as it has recently done with the Morita Baylis-Hillman reaction.²³

Computational details

All calculations were carried out using the hybrid B3LYP functional²⁴ under the density functional theory framework with the Gaussian09 program package.²⁵ We used the standard basis set for organic compounds 6-31G* which include polarization functions for all atoms except H.²⁶ Several other functionals and basis sets were also tested without relevant differences in the results. All geometry optimizations were computed in solution applying the SMD implicit solvation model with tetrahydrofuran as solvent ($\epsilon = 7.4257$).²⁷ In addition, frequency calculations were done for all points in order to include ZPE and free energy corrections and verify the stationary points as minima (zero imaginary frequencies) or transition states (one imaginary frequency). We also checked the transition states by relaxing them towards reactants and products or making IRC calculations. In order to allow energy comparison for all computed points we used explicit solvent molecules to ensure tetra-coordination for all lithium intermediates.

Conclusions

We carried out a full theoretical study of the Shapiro reaction in order to understand the regioselectivity of the process. We calculated the whole mechanism, assessing the strong influence of the hydrazine conformation in the initial structure and the relative acidity of internal and external protons. We conclude that modifying the functional group in the internal position, specifically changing the acidity of the internal protons, the regioselectivity could be strongly affected and the internal alkene could be produced as the main isomer. For this reason, the scope of the reaction could be increased leading to a further improvement of the applicability of this transformation.

Acknowledgements

This research has been supported by the Spanish MICINN (CTQ2011-24800). We are also grateful to the Supercomputing Center of Galicia (CESGA) for CPU time allocation.

References

- 1 R. H. Shapiro and M. J. Heath, *J. Am. Chem. Soc.*, 1967, **89**, 5734–5735.
- 2 R. M. Adlington and A. G. M. Barrett, *Acc. Chem. Res.*, 1983, **16**, 55.
- 3 A. R. Chamberlin and S. H. Bloom, in *Organic Reactions*, Wiley & Sons, 1990, vol. 39.
- 4 R. H. Shapiro, in *Organic Reactions*, ed. W. G. Dauben, John Wiley & Sons, New York, 1976, vol. 23, pp. 405–507.
- 5 K. Granger and M. L. Snapper, *Eur. J. Org. Chem.*, 2012, 2308–2311.
- 6 D. C. Harrowven, D. D. Pascoe, D. Demurtas and H. O. Bourne, *Angew. Chem., Int. Ed.*, 2005, **44**, 1221–1222.
- 7 C. Zhu and S. P. Cook, *J. Am. Chem. Soc.*, 2012, **134**, 13577–13579.
- 8 K. C. Nicolaou, Z. Yang, J. J. Liu, H. Ueno, P. G. Nantermet, R. K. Guy, C. F. Claiborne, J. Renaud, E. A. Couladouros, K. Paulvannan and E. J. Sorensen, *Nature*, 1994, **367**, 630–634.
- 9 O. P. Törmäkangas, R. J. Toivola, E. K. Karvinen and A. M. P. Koskinen, *Tetrahedron*, 2002, **58**, 2175–2181.
- 10 E. J. Corey and B. E. Roberts, *Tetrahedron Lett.*, 1997, **38**, 8919–8920.
- 11 F. Fabris, A. D. Martin and O. D. Lucchi, *Tetrahedron Lett.*, 1999, **40**, 9121–9124.
- 12 C. Morrill and N. S. Mani, *Org. Lett.*, 2007, **9**, 1505–1508.
- 13 U. Siemeling, B. Neumann and H.-G. Stammer, *J. Org. Chem.*, 1997, **62**, 3407–3408.
- 14 W. J. Kerr, A. J. Morrison, M. Paziicky and T. Weber, *Org. Lett.*, 2012, **14**, 2250–2253.
- 15 K. Maruoka, M. Oishi and H. Yamamoto, *J. Am. Chem. Soc.*, 1996, **118**, 2289–2290.
- 16 H. F. Bettinger, R. Mondal and C. Tönshoff, *Org. Biomol. Chem.*, 2008, **6**, 3000–3004.
- 17 B. R. Ramachandran and L. Pratt, in *Practical Aspects of Computational Chemistry II*, ed. J. Leszczynski and M. K. Shukla, Springer, Netherlands, 2012, pp. 471–510.
- 18 L. M. Pratt, D. Jones, A. Sease, D. Busch, E. Faluade, S. C. Nguyen and B. T. Thanh, *Int. J. Quantum Chem.*, 2009, **109**, 34–42.
- 19 B. Ramachandran, P. Kharidehal, L. M. Pratt, S. Voit, F. N. Okeke and M. Ewan, *J. Phys. Chem. A*, 2010, **114**, 8423–8433.
- 20 J. F. McGarrity and C. A. Ogle, *J. Am. Chem. Soc.*, 1985, **107**, 1805–1810.
- 21 M. F. Lipton and R. H. Shapiro, *J. Org. Chem.*, 1978, **43**, 1409–1413.
- 22 M.-H. Yang, S. S. Matikonda and R. A. Altman, *Org. Lett.*, 2013, **15**, 3894–3897.

- 23 R. E. Plata and D. E. Singleton, *J. Am. Chem. Soc.*, 2015, **137**, 3811–3826.
- 24 A. D. Becke, *J. Chem. Phys.*, 1993, **98**, 5648–5652.
- 25 M. J. Frisch, G. W. Trucks, H. B. Schlegel, G. E. Scuseria, M. A. Robb, J. R. Cheeseman, G. Scalmani, V. Barone, B. Mennucci, G. A. Petersson, H. Nakatsuji, M. Caricato, X. Li, H. P. Hratchian, A. F. Izmaylov, J. Bloino, G. Zheng, J. L. Sonnenberg, M. Hada, M. Ehara, K. Toyota, R. Fukuda, J. Hasegawa, M. Ishida, T. Nakajima, Y. Honda, O. Kitao, H. Nakai, T. Vreven, J. A. Montgomery Jr, J. E. Peralta, F. Ogliaro, M. Bearpark, J. J. Heyd, E. Brothers, K. N. Kudin, V. N. Staroverov, R. Kobayashi, J. Normand, K. Raghavachari, A. Rendell, J. C. Burant, S. S. Iyengar, J. Tomasi, M. Cossi, N. Rega, J. M. Millam, M. Klene, J. E. Knox, J. B. Cross, V. Bakken, C. Adamo, J. Jaramillo, R. Gomperts, R. E. Stratmann, O. Yazyev, A. J. Austin, R. Cammi, C. Pomelli, J. W. Ochterski, R. L. Martin, K. Morokuma, V. G. Zakrzewski, G. A. Voth, P. Salvador, J. J. Dannenberg, S. Dapprich, A. D. Daniels, Ö. Farkas, J. B. Foresman, J. V. Ortiz, J. Cioslowski and D. J. Fox, *R. A. Gaussian 09*, Gaussian, Inc., Wallingford CT, 2009.
- 26 P. C. Hariharan and J. A. Pople, *Theor. Chim. Acta*, 1973, **28**, 213–222.
- 27 A. V. Marenich, C. J. Cramer and D. G. Truhlar, *J. Phys. Chem. B*, 2009, **113**, 6378–6396.